Spectral properties of a double-quantum-dot structure: A causal Green's function approach

J. Q. You* and Hou-Zhi Zheng
National Laboratory for Superlattices and Microstructures, Institute of Semiconductors, Chinese Academy of Sciences, P.O. Box 912, Beijing 100083, China

(Received 13 January 1999; revised manuscript received 15 April 1999)

Spectral properties of a double quantum dot (QD) structure are studied by a causal Green's function (GF) approach. The double QD system is modeled by an Anderson-type Hamiltonian in which both the intra- and interdot Coulomb interactions are taken into account. The GF's are derived by an equation-of-motion method and the real-space renormalization-group technique. The numerical results show that the average occupation number of electrons in the QD exhibits staircase features and the local density of states depends appreciably on the electron occupation of the dot. [S0163-1829(99)12535-9]

I. INTRODUCTION

Semiconductor quantum dots (QD's) are nanostructures that allow electronic properties to be tailored through quantum confinement. In these systems, the discreteness of charge carried by a single electron and the interplay of quantum effects become manifest in striking ways.[1] Now, advances in nanotechnologies have made it feasible to realize tunneling through a single electronic level within the dot. Because the Coulomb interaction of electrons is important in the QD, several theoretical papers[2–6] have suggested that the tunneling through this single quantum level can be appropriately described by the Anderson model for a single magnetic impurity.

Recently, increasing interest has been generated in double QD structures.[1,7–10] As compared with the single-dot structure, the double QD system exhibits more complex behaviors and has, however, been less investigated due to its complexity. Very recently, Fujisawa *et al.*[9] experimentally studied the inelastic transitions in a double QD system, and Blick *et al.*[10] performed photoconductive measurements on the double QD and demonstrated the Rabi oscillations in this artificial molecule. These studies show that the energy spectrum of the double QD strucure is essential in understanding the experimental observations.

In the present article, we investigate the spectral properties of the double QD system by a causal Green's function (GF) approach. The double QD structure we study is modeled as two coupled QD's, each connected via a tunnel barrier to a lead. As in Refs. 7 and 8, to reveal the effects of electron correlations, we employ an Anderson-type Hamiltonian to model the double QD system, where both the intra and interdot Coulomb interactions are taken into account. The paper is organized as follows: In Sec. II, the causal GF's are studied. We derive the GF's by an equation-of-motion method and the real-space renormalization-group (RG) technique. In Sec. III, we present the numerical results on the electron occupation and the local density of states (LDOS) of the double QD structure. The electron occupation of the QD is calculated in a self-consistent way. Finally, Sec. IV provides a brief summary of the paper.

II. CAUSAL GREEN'S FUNCTIONS

For the double-QD structure, we consider an Anderson-type model in the tight-binding formalism

$$H = H_d + H_t + H_0, \tag{1}$$

with

$$H_d = \sum_{\sigma} \left[E_A c^{\dagger}_{A\sigma} c_{A\sigma} + E_B c^{\dagger}_{B\sigma} c_{B\sigma} + T_{AB} (c^{\dagger}_{A\sigma} c_{B\sigma} + \text{H.c.}) \right] + U_A n_{A\uparrow} n_{A\downarrow} + U_B n_{B\uparrow} n_{B\downarrow} + V_{AB} \sum_{\sigma\sigma'} n_{A\sigma} n_{B\sigma'}, \tag{2}$$

$$H_t = T_L \sum_{\sigma} (c^{\dagger}_{A\sigma} c_{\alpha\sigma} + \text{H.c.}) + T_R \sum_{\sigma} (c^{\dagger}_{B\sigma} c_{\beta\sigma} + \text{H.c.}), \tag{3}$$

and

$$H_0 = \sum_{i,\sigma} \left[\varepsilon_i c^{\dagger}_{i\sigma} c_{i\sigma} + t_l (c^{\dagger}_{i\sigma} c_{i-1,\sigma} + \text{H.c.}) \right] + \sum_{j,\sigma} \left[\varepsilon_j c^{\dagger}_{j\sigma} c_{j\sigma} + t_r (c^{\dagger}_{j\sigma} c_{j+1,\sigma} + \text{H.c.}) \right]. \tag{4}$$

Here, H_d is the Hamiltonian of an isolated double QD, in which $n_{A\sigma}$ ($n_{B\sigma}$) is the number operator for electrons with spin σ in dot A (B). The term $U_A n_{A\uparrow} n_{A\downarrow}$ ($U_B n_{B\uparrow} n_{B\downarrow}$) in Eq. (2) characterizes the effect of Coulomb interaction between two electrons of different spins in dot A (B), while the last term in Eq. (2) characterizes the effect of interdot Coulomb interaction.[7,8] The Hamiltonian H_t describes the transfer of electrons between the left lead and dot A, and between the right lead and dot B. Typically, U_A and U_B are much larger than the transfer integrals $|T_L|$, $|T_R|$, and $|T_{AB}|$ in the double QD structure. Equation (4) gives the Hamiltonian of the left and right leads, where $\varepsilon_i = \varepsilon_\alpha$ for site $i = \alpha$ and $\varepsilon_i = \varepsilon_l$ for sites $i = -1, -2, -3, \ldots$, while $\varepsilon_j = \varepsilon_\beta$ for site $j = \beta$ and $\varepsilon_j = \varepsilon_r$ for sites $j = 1,2,3, \ldots$. In the following, we employ the causal GF's to obtain the spectral properties of the model Hamiltonian (1).

The retarded GF for Fermi operators C and D is defined as

$$G(t)=-\frac{i}{\hbar}\theta(t)\langle\{C(t),D\}\rangle=\langle\langle C(t);D\rangle\rangle, \tag{5}$$

where $\theta(t)$ is the Heaviside function, the curly brackets denote the anticommutator, and the brakets $\langle\cdots\rangle$ indicate the thermal average. The Fourier transform of $G(t)$

$$G(Z)=\int_{-\infty}^{\infty}dtG(t)\exp(iZt/\hbar)=\langle\langle C|D\rangle\rangle \tag{6}$$

obeys the equation of motion[11,12]

$$Z\langle\langle C|D\rangle\rangle=\langle\{C,D\}\rangle+\langle\langle[C,H]|D\rangle\rangle, \tag{7}$$

where $Z=E+i\eta$, with η being a positive infinitesimal number.

From Eq. (7) it follows that

$$\begin{aligned}(Z-E_A)\langle\langle c_{A\sigma}|c_{A\sigma}^{\dagger}\rangle\rangle=1&+T_{AB}\langle\langle c_{B\sigma}|c_{A\sigma}^{\dagger}\rangle\rangle+T_L\langle\langle c_{\alpha\sigma}|c_{A\sigma}^{\dagger}\rangle\rangle\\&+U_A\langle\langle n_{A\bar{\sigma}}c_{A\sigma}|c_{A\sigma}^{\dagger}\rangle\rangle\\&+V_{AB}(\langle\langle n_{B\sigma}c_{A\sigma}|c_{A\sigma}^{\dagger}\rangle\rangle\\&+\langle\langle n_{B\bar{\sigma}}c_{A\sigma}|c_{A\sigma}^{\dagger}\rangle\rangle),\end{aligned} \tag{8}$$

where $\langle\langle n_{A\bar{\sigma}}c_{A\sigma}|c_{A\sigma}^{\dagger}\rangle\rangle$, $\langle\langle n_{B\sigma}c_{A\sigma}|c_{A\sigma}^{\dagger}\rangle\rangle$, and $\langle\langle n_{B\bar{\sigma}}c_{A\sigma}|c_{A\sigma}^{\dagger}\rangle\rangle$ satisfy

$$\begin{aligned}Z\langle\langle n_{A\bar{\sigma}}c_{A\sigma}|c_{A\sigma}^{\dagger}\rangle\rangle&=\langle n_{A\bar{\sigma}}\rangle+\langle\langle[n_{A\bar{\sigma}}c_{A\sigma},H]|c_{A\sigma}^{\dagger}\rangle\rangle,\\Z\langle\langle n_{B\sigma}c_{A\sigma}|c_{A\sigma}^{\dagger}\rangle\rangle&=\langle n_{B\sigma}\rangle+\langle\langle[n_{B\sigma}c_{A\sigma},H]|c_{A\sigma}^{\dagger}\rangle\rangle,\\Z\langle\langle n_{B\bar{\sigma}}c_{A\sigma}|c_{A\sigma}^{\dagger}\rangle\rangle&=\langle n_{B\bar{\sigma}}\rangle+\langle\langle[n_{B\bar{\sigma}}c_{A\sigma},H]|c_{A\sigma}^{\dagger}\rangle\rangle.\end{aligned} \tag{9}$$

Since correlation between electrons at the same site is of dominant importance, we follow Hubbard[13] to approximate GF's involving more than two sites by GF's involving not more than two sites. Here $[n_{A\bar{\sigma}}c_{A\sigma},H]$, $[n_{B\sigma}c_{A\sigma},H]$, and $[n_{B\bar{\sigma}}c_{A\sigma},H]$ are approximated by

$$\begin{aligned}[n_{A\bar{\sigma}}c_{A\sigma},H]=&(E_A+U_A)n_{A\bar{\sigma}}c_{A\sigma}+\langle n_{A\bar{\sigma}}\rangle(T_{AB}c_{B\sigma}+T_Lc_{\alpha\sigma})\\&+V_{AB}(n_{A\bar{\sigma}}n_{B\sigma}c_{A\sigma}+n_{A\bar{\sigma}}n_{B\bar{\sigma}}c_{A\sigma}),\end{aligned} \tag{10}$$

$$\begin{aligned}[n_{B\sigma}c_{A\sigma},H]=&[E_A+V_{AB}(1+\langle n_{B\bar{\sigma}}\rangle)]n_{B\sigma}c_{A\sigma}+\langle n_{B\sigma}\rangle\\&\times(T_{AB}c_{B\sigma}+T_Lc_{\alpha\sigma})+U_An_{A\bar{\sigma}}n_{B\sigma}c_{A\sigma},\end{aligned} \tag{11}$$

$$\begin{aligned}[n_{B\bar{\sigma}}c_{A\sigma},H]=&[E_A+V_{AB}(1+\langle n_{B\sigma}\rangle)]n_{B\bar{\sigma}}c_{A\sigma}+\langle n_{B\bar{\sigma}}\rangle\\&\times(T_{AB}c_{B\sigma}+T_Lc_{\alpha\sigma})+U_An_{A\bar{\sigma}}n_{B\bar{\sigma}}c_{A\sigma}.\end{aligned} \tag{12}$$

Substitution of Eqs. (10)-(12) into Eq. (9) gives

$$\begin{aligned}&(Z-E_A-U_A)\langle\langle n_{A\bar{\sigma}}c_{A\sigma}|c_{A\sigma}^{\dagger}\rangle\rangle\\&\quad=\langle n_{A\bar{\sigma}}\rangle(1+T_{AB}\langle\langle c_{B\sigma}|c_{A\sigma}^{\dagger}\rangle\rangle+T_L\langle\langle c_{\alpha\sigma}|c_{A\sigma}^{\dagger}\rangle\rangle)\\&\qquad+V_{AB}(\langle\langle n_{A\bar{\sigma}}n_{B\sigma}c_{A\sigma}|c_{A\sigma}^{\dagger}\rangle\rangle+\langle\langle n_{A\bar{\sigma}}n_{B\bar{\sigma}}c_{A\sigma}|c_{A\sigma}^{\dagger}\rangle\rangle),\end{aligned} \tag{13}$$

$$\begin{aligned}&[Z-E_A-V_{AB}(1+\langle n_{B\bar{\sigma}}\rangle)]\langle\langle n_{B\sigma}c_{A\sigma}|c_{A\sigma}^{\dagger}\rangle\rangle\\&\quad=\langle n_{B\sigma}\rangle(1+T_{AB}\langle\langle c_{B\sigma}|c_{A\sigma}^{\dagger}\rangle\rangle+T_L\langle\langle c_{\alpha\sigma}|c_{A\sigma}^{\dagger}\rangle\rangle)\\&\qquad+U_A\langle\langle n_{A\bar{\sigma}}n_{B\sigma}c_{A\sigma}|c_{A\sigma}^{\dagger}\rangle\rangle,\end{aligned} \tag{14}$$

$$\begin{aligned}&[Z-E_A-V_{AB}(1+\langle n_{B\sigma}\rangle)]\langle\langle n_{B\bar{\sigma}}c_{A\sigma}|c_{A\sigma}^{\dagger}\rangle\rangle\\&\quad=\langle n_{B\bar{\sigma}}\rangle(1+T_{AB}\langle\langle c_{B\sigma}|c_{A\sigma}^{\dagger}\rangle\rangle+T_L\langle\langle c_{\alpha\sigma}|c_{A\sigma}^{\dagger}\rangle\rangle)\\&\qquad+U_A\langle\langle n_{A\bar{\sigma}}n_{B\bar{\sigma}}c_{A\sigma}|c_{A\sigma}^{\dagger}\rangle\rangle.\end{aligned} \tag{15}$$

The above equations of motion are not closed, since the third-order GF's $\langle\langle n_{A\bar{\sigma}}n_{B\sigma}c_{A\sigma}|c_{A\sigma}^{\dagger}\rangle\rangle$ and $\langle\langle n_{A\bar{\sigma}}n_{B\bar{\sigma}}c_{A\sigma}|c_{A\sigma}^{\dagger}\rangle\rangle$ are needed to derive the second-order GF's $\langle\langle n_{A\bar{\sigma}}c_{A\sigma}|c_{A\sigma}^{\dagger}\rangle\rangle$, $\langle\langle n_{B\sigma}c_{A\sigma}|c_{A\sigma}^{\dagger}\rangle\rangle$, and $\langle\langle n_{B\bar{\sigma}}c_{A\sigma}|c_{A\sigma}^{\dagger}\rangle\rangle$. Writing the equations of motion for the third-order GF's and closing them at this stage, we obtain the following relations:

$$\begin{aligned}&\langle\langle n_{A\bar{\sigma}}n_{B\sigma}c_{A\sigma}|c_{A\sigma}^{\dagger}\rangle\rangle\\&\quad=\frac{\langle n_{A\bar{\sigma}}\rangle\langle n_{B\sigma}\rangle}{Z-E_A-U_A-V_{AB}(1+\langle n_{B\bar{\sigma}}\rangle)}(1+T_{AB}\langle\langle c_{B\sigma}|c_{A\sigma}^{\dagger}\rangle\rangle\\&\qquad+T_L\langle\langle c_{\alpha\sigma}|c_{A\sigma}^{\dagger}\rangle\rangle),\end{aligned} \tag{16}$$

$$\begin{aligned}&\langle\langle n_{A\bar{\sigma}}n_{B\bar{\sigma}}c_{A\sigma}|c_{A\sigma}^{\dagger}\rangle\rangle\\&\quad=\frac{\langle n_{A\bar{\sigma}}\rangle\langle n_{B\bar{\sigma}}\rangle}{Z-E_A-U_A-V_{AB}(1+\langle n_{B\sigma}\rangle)}(1+T_{AB}\langle\langle c_{B\sigma}|c_{A\sigma}^{\dagger}\rangle\rangle\\&\qquad+T_L\langle\langle c_{\alpha\sigma}|c_{A\sigma}^{\dagger}\rangle\rangle).\end{aligned} \tag{17}$$

From Eqs. (8) and (13)-(17), we finally obtain

$$\langle\langle c_{A\sigma}|c_{A\sigma}^{\dagger}\rangle\rangle=g_{A\sigma}(1+T_{AB}\langle\langle c_{B\sigma}|c_{A\sigma}^{\dagger}\rangle\rangle+T_L\langle\langle c_{\alpha\sigma}|c_{A\sigma}^{\dagger}\rangle\rangle), \tag{18}$$

with

$$\begin{aligned}g_{A\sigma}(Z)=g_{A\sigma}^{(0)}(Z)+\frac{V_{AB}}{Z-E_A}\Bigg[&g_{A\sigma}^{(1)}(Z)+g_{A\sigma}^{(2)}(Z)\\&+\frac{U_A}{Z-E_A-U_A}g_{A\sigma}^{(3)}(Z)\Bigg],\end{aligned} \tag{19}$$

where $g_{A\sigma}^{(i)}(Z)$, $i=0$, 1, 2, and 3, are given by

$$g_{A\sigma}^{(0)}(Z)=\frac{1-\langle n_{A\bar{\sigma}}\rangle}{Z-E_A}+\frac{\langle n_{A\bar{\sigma}}\rangle}{Z-E_A-U_A}. \tag{20}$$

$$\begin{aligned}g_{A\sigma}^{(1)}(Z)=&\frac{(1-\langle n_{A\bar{\sigma}}\rangle)\langle n_{B\sigma}\rangle}{Z-E_A-V_{AB}(1+\langle n_{B\bar{\sigma}}\rangle)}\\&+\frac{\langle n_{A\bar{\sigma}}\rangle\langle n_{B\sigma}\rangle}{Z-E_A-U_A-V_{AB}(1+\langle n_{B\bar{\sigma}}\rangle)},\end{aligned} \tag{21}$$

$$\begin{aligned}g_{A\sigma}^{(2)}(Z)=&\frac{(1-\langle n_{A\bar{\sigma}}\rangle)\langle n_{B\bar{\sigma}}\rangle}{Z-E_A-V_{AB}(1+\langle n_{B\sigma}\rangle)}\\&+\frac{\langle n_{A\bar{\sigma}}\rangle\langle n_{B\bar{\sigma}}\rangle}{Z-E_A-U_A-V_{AB}(1+\langle n_{B\sigma}\rangle)},\end{aligned} \tag{22}$$

$$g^{(3)}_{A\sigma}(Z)=\frac{\langle n_{A\bar{\sigma}}\rangle\langle n_{B\sigma}\rangle}{Z-E_A-U_A-V_{AB}(1+\langle n_{B\bar{\sigma}}\rangle)}+\frac{\langle n_{A\bar{\sigma}}\rangle\langle n_{B\bar{\sigma}}\rangle}{Z-E_A-U_A-V_{AB}(1+\langle n_{B\sigma}\rangle)}. \quad (23)$$

A similar decoupling approximation was also employed in Ref. 2 to derive the retarded GF of a single QD system. This kind of decoupling approximation is valid for temperatures higher than the Kondo temperature.[14,15] Analogously, one can derive the following equations:

$$\langle\langle c_{A\sigma}|c^{\dagger}_{B\sigma}\rangle\rangle=g_{A\sigma}(T_{AB}\langle\langle c_{B\sigma}|c^{\dagger}_{B\sigma}\rangle\rangle+T_L\langle\langle c_{\alpha\sigma}|c^{\dagger}_{B\sigma}\rangle\rangle), \quad (24)$$

$$\langle\langle c_{B\sigma}|c^{\dagger}_{B\sigma}\rangle\rangle=g_{B\sigma}(1+T_{AB}\langle\langle c_{A\sigma}|c^{\dagger}_{B\sigma}\rangle\rangle+T_R\langle\langle c_{\beta\sigma}|c^{\dagger}_{B\sigma}\rangle\rangle), \quad (25)$$

$$\langle\langle c_{B\sigma}|c^{\dagger}_{A\sigma}\rangle\rangle=g_{B\sigma}(T_{AB}\langle\langle c_{A\sigma}|c^{\dagger}_{A\sigma}\rangle\rangle+T_R\langle\langle c_{\beta\sigma}|c^{\dagger}_{A\sigma}\rangle\rangle), \quad (26)$$

with $g_{B\sigma}(Z)$ given by

$$g_{B\sigma}(Z)=g^{(0)}_{B\sigma}(Z)+\frac{V_{BA}}{Z-E_B}\left[g^{(1)}_{B\sigma}(Z)+g^{(2)}_{B\sigma}(Z)+\frac{U_B}{Z-E_B-U_B}g^{(3)}_{B\sigma}(Z)\right]. \quad (27)$$

Here, $V_{BA}=V_{AB}$ and $g^{(i)}_{B\sigma}(Z)$, $i=0$, 1, 2, and 3, are obtained from Eqs. (20)-(23) by replacing A (B) with B (A).

Also, it follows from Eq. (7) that

$$(Z-\varepsilon_\beta)\langle\langle c_{\beta\sigma}|c^{\dagger}_{B\sigma}\rangle\rangle=T_R\langle\langle c_{B\sigma}|c^{\dagger}_{B\sigma}\rangle\rangle+t_r\langle\langle c_{1\sigma}|c^{\dagger}_{B\sigma}\rangle\rangle,$$

$$(Z-\varepsilon_r)\langle\langle c_{j\sigma}|c^{\dagger}_{B\sigma}\rangle\rangle=t_r\langle\langle c_{j-1,\sigma}|c^{\dagger}_{B\sigma}\rangle\rangle+t_r\langle\langle c_{j+1,\sigma}|c^{\dagger}_{B\sigma}\rangle\rangle,$$

$$j=1,2,3,\ldots. \quad (28)$$

This set of equations can be solved effeciently by the real-space RG technique.[16,17] As odd sites are decimated, one obtains a new semi-infinite lattice with renormalized parameters. At the nth stage of decimation, Eq. (28) becomes

$$(Z-\varepsilon^{(n)}_\beta)\langle\langle c_{\beta\sigma}|c^{\dagger}_{B\sigma}\rangle\rangle=T_R\langle\langle c_{B\sigma}|c^{\dagger}_{B\sigma}\rangle\rangle+t^{(n)}_r\langle\langle c_{2^n,\sigma}|c^{\dagger}_{B\sigma}\rangle\rangle,$$

$$(Z-\varepsilon^{(n)}_r)\langle\langle c_{2^nj,\sigma}|c^{\dagger}_{B\sigma}\rangle\rangle=t^{(n)}_r\langle\langle c_{2^n(j-1),\sigma}|c^{\dagger}_{B\sigma}\rangle\rangle+t^{(n)}_r\langle\langle c_{2^n(j+1),\sigma}|c^{\dagger}_{B\sigma}\rangle\rangle,$$

$$j=1,2,3,\ldots, \quad (29)$$

where the RG equations are

$$t^{(n)}_r=\frac{(t^{(n-1)}_r)^2}{Z-\varepsilon^{(n-1)}_r},\quad \varepsilon^{(n)}_r=\varepsilon^{(n-1)}_r+2t^{(n)}_r,$$

$$\varepsilon^{(n)}_\beta=\varepsilon^{(n-1)}_\beta+t^{(n)}_r,\quad n=1,2,3,\ldots, \quad (30)$$

with $t^{(0)}_r=t_r$, $\varepsilon^{(0)}_r=\varepsilon_r$, and $\varepsilon^{(0)}_\beta=\varepsilon_\beta$. When $n\to\infty$, there is $t^{(n)}_r\to 0$, and then $\varepsilon^{(n)}_r\to\varepsilon^*_r$ and $\varepsilon^{(n)}_\beta\to\varepsilon^*_\beta$, where ε^*_r and ε^*_β correspond to the fixed point of the RG equations. In the numerical calculations, tens of iterations are adequate because the RG equations converge to the fixed point rapidly with increasing iterations. Thus, we have

$$\langle\langle c_{\beta\sigma}|c^{\dagger}_{B\sigma}\rangle\rangle=\frac{T_R}{Z-\varepsilon^*_\beta}\langle\langle c_{B\sigma}|c^{\dagger}_{B\sigma}\rangle\rangle. \quad (31)$$

Similarly, one can derive that

$$\langle\langle c_{\beta\sigma}|c^{\dagger}_{A\sigma}\rangle\rangle=\frac{T_R}{Z-\varepsilon^*_\beta}\langle\langle c_{B\sigma}|c^{\dagger}_{A\sigma}\rangle\rangle, \quad (32)$$

$$\langle\langle c_{\alpha\sigma}|c^{\dagger}_{A\sigma}\rangle\rangle=\frac{T_L}{Z-\varepsilon^*_\alpha}\langle\langle c_{A\sigma}|c^{\dagger}_{A\sigma}\rangle\rangle, \quad (33)$$

$$\langle\langle c_{\alpha\sigma}|c^{\dagger}_{B\sigma}\rangle\rangle=\frac{T_L}{Z-\varepsilon^*_\alpha}\langle\langle c_{A\sigma}|c^{\dagger}_{B\sigma}\rangle\rangle, \quad (34)$$

where ε^*_α corresponds to the fixed point of the RG equations that have the same form as Eq. (30) with substitutions of α and l for β and r.

Substituting Eqs. (31)-(34) into Eqs. (18) and (24)-(26), we finally obtain the solutions for the GF's:

$$\langle\langle c_{A\sigma}|c^{\dagger}_{A\sigma}\rangle\rangle=\frac{G^{(0)}_{A\sigma}}{1-G^{(0)}_{A\sigma}G^{(0)}_{B\sigma}T^2_{AB}},$$

$$\langle\langle c_{B\sigma}|c^{\dagger}_{B\sigma}\rangle\rangle=\frac{G^{(0)}_{B\sigma}}{1-G^{(0)}_{A\sigma}G^{(0)}_{B\sigma}T^2_{AB}},$$

$$\langle\langle c_{A\sigma}|c^{\dagger}_{B\sigma}\rangle\rangle=\langle\langle c_{B\sigma}|c^{\dagger}_{A\sigma}\rangle\rangle=\frac{G^{(0)}_{A\sigma}G^{(0)}_{B\sigma}T_{AB}}{1-G^{(0)}_{A\sigma}G^{(0)}_{B\sigma}T^2_{AB}}, \quad (35)$$

where

$$G^{(0)}_{A\sigma}(Z)=\frac{g_{A\sigma}}{1-g_{A\sigma}T^2_L/(Z-\varepsilon^*_\alpha)},$$

$$G^{(0)}_{B\sigma}(Z)=\frac{g_{B\sigma}}{1-g_{B\sigma}T^2_R/(Z-\varepsilon^*_\beta)}, \quad (36)$$

in which $g_{A\sigma}(Z)$ and $g_{B\sigma}(Z)$ are given by Eqs. (19) and (27).

III. ELECTRON OCCUPATION AND LOCAL DENSITY OF STATES

The average occupation numbers of electrons in dots A and B are given by

$$\langle n_{A\sigma}\rangle=\langle c^{\dagger}_{A\sigma}c_{A\sigma}\rangle=\int_{-\infty}^{\infty}dEf(E)\rho_{A\sigma}(E),$$

$$\langle n_{B\sigma}\rangle=\langle c^{\dagger}_{B\sigma}c_{B\sigma}\rangle=\int_{-\infty}^{\infty}dEf(E)\rho_{B\sigma}(E), \quad (37)$$

where $f(E)=\{\exp[(E-\mu)/k_BT]+1\}^{-1}$ is the Fermi distribution and the LDOS's for dots A and B are determined by the retarded GF's:

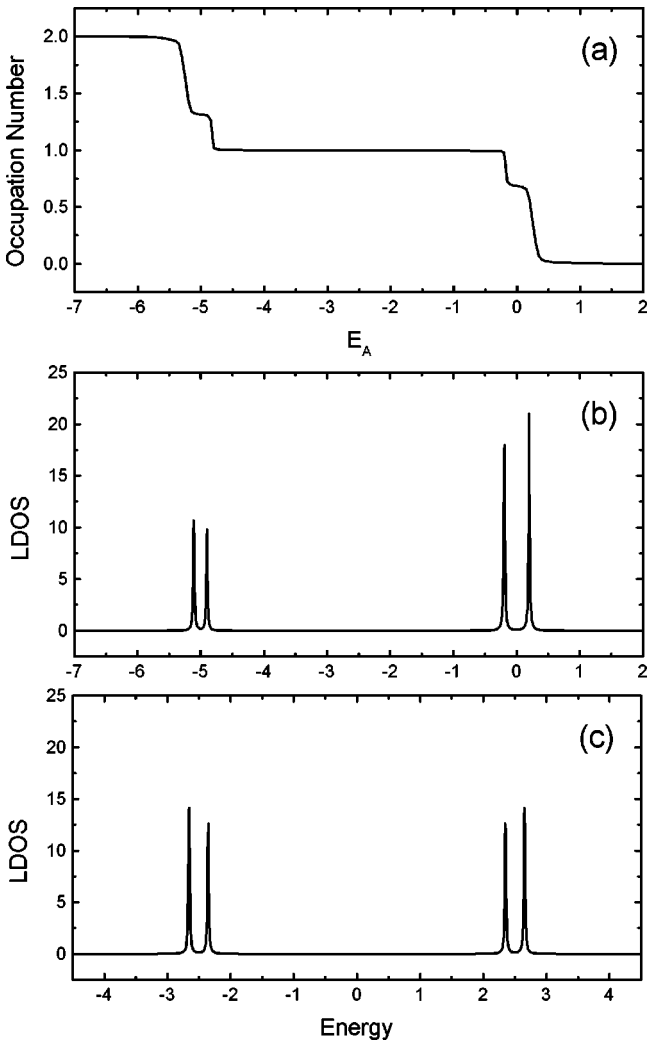

FIG. 1. (a) Average occupation number n_A as a function of the site energy E_A; (b) and (c) LDOS at dot A for $E_A=$ (b) -5 and (c) -2.5. Here, $V_{AB}=0$, $T_{AB}=-0.3$, $k_BT=0.01$, and $\mu=0$. In this figure and the following ones, we choose $U_A=U_B=5$, $T_L=T_R=-0.1$, $\varepsilon_l=\varepsilon_r=\varepsilon_\alpha=\varepsilon_\beta=0$, and $t_l=t_r=-30$.

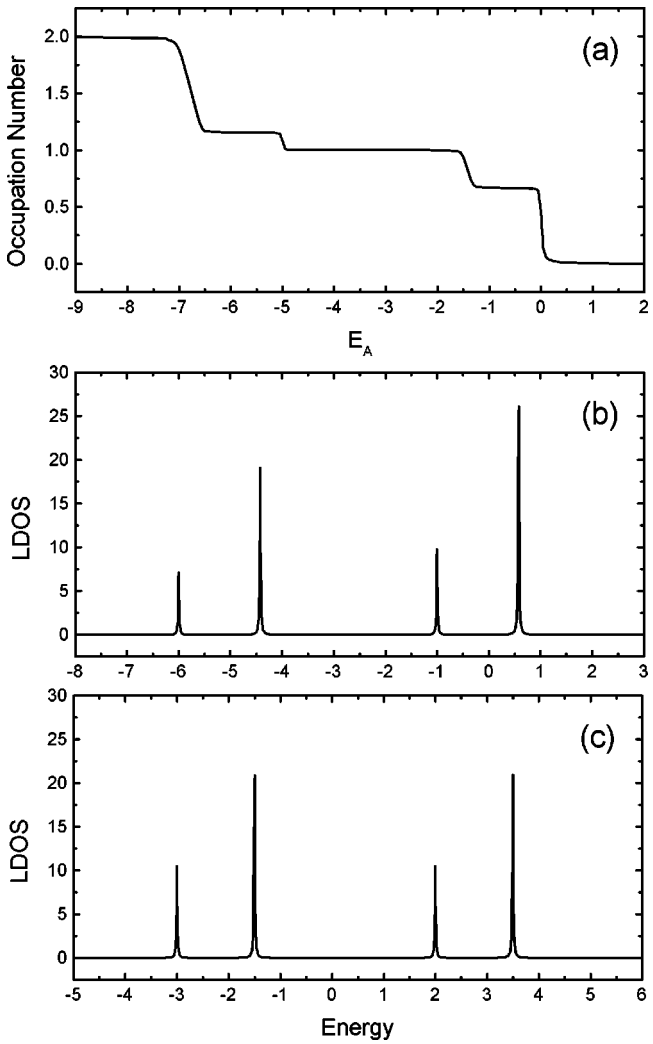

FIG. 2. (a) Average occupation number n_A as a function of the site energy E_A; (b) and (c) LDOS at dot A for $E_A=$ (b) -6 and (c) -3. Here, $V_{AB}=1$, $T_{AB}=0$, $k_BT=0.01$, and $\mu=0$. Other parameters are the same as in Fig. 1.

$$\rho_{A\sigma}(E)=-\frac{1}{\pi}\mathrm{Im}\langle\langle c_{A\sigma}|c_{A\sigma}^{\dagger}\rangle\rangle,$$

$$\rho_{B\sigma}(E)=-\frac{1}{\pi}\mathrm{Im}\langle\langle c_{B\sigma}|c_{B\sigma}^{\dagger}\rangle\rangle. \tag{38}$$

Since the retarded GF's $\langle\langle c_{A\sigma}|c_{A\sigma}^{\dagger}\rangle\rangle$ and $\langle\langle c_{B\sigma}|c_{B\sigma}^{\dagger}\rangle\rangle$ depend on $\langle n_{A\bar{\sigma}}\rangle$ and $\langle n_{B\bar{\sigma}}\rangle$ through $g_{A\sigma}(Z)$ and $g_{B\sigma}(Z)$, the average occupation numbers $\langle n_{A\sigma}\rangle$ and $\langle n_{B\sigma}\rangle$ are thus determined self-consistently.

In what follows, we present the numerical calculations. As a typical example, we study the symmetric double-QD structures with parameters: $E_A=E_B$, $U_A=U_B$, $T_L=T_R$, $\varepsilon_l=\varepsilon_r=\varepsilon_\alpha=\varepsilon_\beta=0$, and $t_l=t_r=-30$. Here the nonmagnetic case is considered, i.e., $\langle n_{A\uparrow}\rangle=\langle n_{A\downarrow}\rangle$ and $\langle n_{B\uparrow}\rangle=\langle n_{B\downarrow}\rangle$; for the symmetric structures, one further has $\langle n_{A\uparrow}\rangle=\langle n_{A\downarrow}\rangle=\langle n_{B\uparrow}\rangle=\langle n_{B\downarrow}\rangle$. Recently, Pohjola *et al.*[8] studied the Kondo effect in the double-QD structure. This is not the case we study, since temperatures higher than the Kondo one are here involved.

Figure 1(a) presents the average occupation number of electrons in dot A, $n_A=\langle n_{A\uparrow}\rangle+\langle n_{A\downarrow}\rangle$, as a function of the site energy E_A (the single-particle level of the dot A). The parameters are chosen to be $U_A=U_B=5$, $V_{AB}=0$, $T_{AB}=-0.3$, and $T_L=T_R=-0.1$. The temperature is $k_BT=0.01$ and the chemical potential is fixed at $\mu=0$. It can be seen that with the site energy decreasing, which is equivalent to the uplift of the chemical potential, the average occupation number increases in a staircase fashion. Interestingly, two small steps appear around $E_A=0$ (-5). As explained below, these two steps are due to the occurrence of the spectral splittings at single-dot levels E_A and E_A+U_A. In the present case, the interdot Coulomb interaction is not considered $(V_{AB}=0)$. If the interdot and dot-lead couplings are further removed, the dots A and B become two isolated QD's. For the symmetric structure we study, each isolated dot has levels $E_A=E_B$ and $E_A+U_A=E_B+U_B$. It is expected that the presence of the interdot coupling will split each of the degenerate levels $E_A=E_B$ and $E_A+U_A=E_B+U_B$ into two molecular ones, while the couplings between dots and leads will modify (renormalize) the molecular states. Because the chemical potential is kept zero, the decrease of the single-

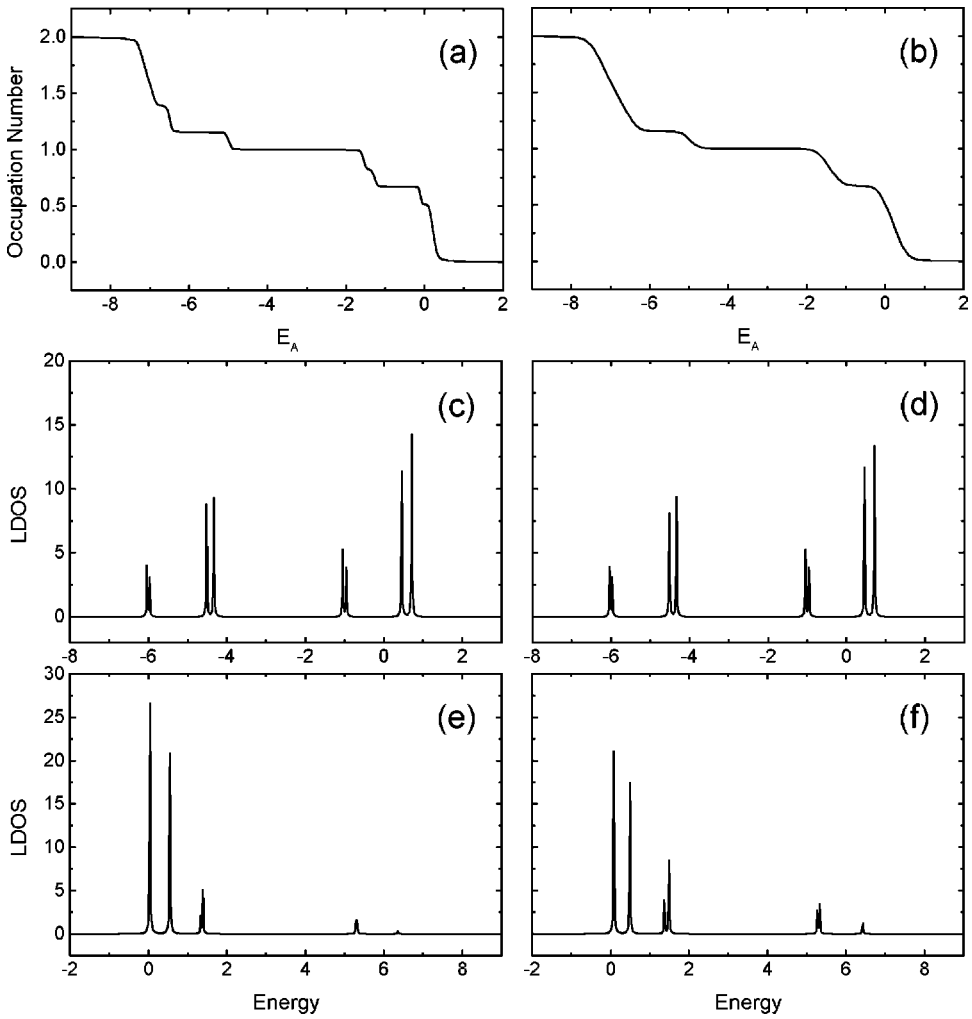

FIG. 3. (a) and (b) Average occupation number n_A as a function of the site energy E_A for $k_BT=$ (a) 0.01 and (b) 0.1; (c) and (d) LDOS at dot A for $E_A=-6$, where $k_BT=$ (c) 0.01 and (d) 0.1; (e) and (f) LDOS at dot A for $E_A=0.3$, where $k_BT=$ (e) 0.01 and (f) 0.1. Here $V_{AB}=1$, $T_{AB}=-0.3$, and $\mu=0$. Other parameters are the same as in Fig. 1.

particle level E_A $(=E_B)$ then leads to the successive filling of the renormalized molecular levels and yields a steplike variation of the electron occupation. The staircase feature of the average occupation number displayed in Fig. 1(a) is similar to the results derived by directly diagonalizing the Hamiltonian of the system with a given number of electrons.[7] However, our results show that the heights of the two small steps around $E_A=0$ (-5) are different, which indicates that the probabilities of electron occupancy on the renormalized molecular states are not the same. In our work, an infinite system is actually treated, since the spectral properties of the double QD are derived from the total Hamiltonian that includes the dot-lead couplings. The unequal step heights described above may be due to the renormalization effect by the couplings between dots and leads. In Figs. 1(b) and 1(c), we display the LDOS at dot A, $\rho_A=\rho_{A\uparrow}+\rho_{A\downarrow}$, for $E_A=-5$ and -2.5. The LDOS exhibits a four-peak structure in which a gap, determined mainly by the Coulomb interaction, separates the two LDOS peaks at lower energies and the two peaks at higher energies. When the site energy E_A increases, the two LDOS peaks at lower energies increase in both height and spectral splitting, while the other two peaks at higher energies decreases in both height and spectral splitting. Since the shift of the site energy E_A is associated with the variation of the average occupation number [see Fig. 1(a)], the above observations indicate that the LDOS depends sensitively upon the electron occupation of the dot. In the noninteracting case, the two peaks at higher energies disappear and the two peaks at lower energies correspond to the single-particle levels of the double QD. The dependence of the LDOS peak heights and positions on the electron occupation reveals that the single-particle spectrum is appreciably affected by the Coulomb interaction. Also, from Fig. 1(c) it can be seen that at $E_A=-2.5$, the LDOS is symmetric about $E=0$ (the position of the chemical potential). This corresponds to the half filling of the QD, since there is $\langle n_{A\uparrow}\rangle=\langle n_{A\downarrow}\rangle=0.5$.

In Fig. 2, we show the average occupation number of electrons in dot A and the LDOS for the case of $T_{AB}=0$ and $V_{AB}=1$. Analogous to Fig. 1, the average occupation number of electrons exhibits staircase features. Also, the LDOS has a four-peak structure and depends appreciably on the variation of the site energy E_A. If the dot-lead couplings are further absent, the dots A and B are then connected only by the interdot Coulomb interaction. Associated with all possible occupancy configurations of the isolated double QD, the electrons in dot A take four kinds of levels, E_A, E_A+V_{AB}, E_A+U_A, and $E_A+U_A+V_{AB}$, while the electrons in dot B take levels, E_B, E_B+V_{AB}, E_B+U_B, and $E_B+U_B+V_{AB}$, in which only E_A and E_B are the single-particle levels. For the symmetric structure, these levels are degenerate, i.e., $E_A=E_B$, $E_A+V_{AB}=E_B+V_{AB}$, $E_A+U_A=E_B+U_B$, and $E_A+U_A+V_{AB}=E_B+U_B+V_{AB}$. The four peaks in the

LDOS [see Figs. 2(b) and 2(c)] correspond to these four degenerate levels, but they have been renormalized by the couplings between dots and leads.

Figure 3 displays the average occupation number of electrons in dot A and the LDOS for the case of $T_{AB}=-0.3$ and $V_{AB}=1$. In the LDOS's given in Figs. 2(b) and 2(c), the lowest peak corresponds to the single-particle level. As expected, it will be split into two molecular levels by the presence of the interdot coupling [see, e.g., Fig. 3(c)]. For the other three peaks, the calculated LDOS demonstrates such spectral splittings as well. The spectral splittings are also reflected in the average occupation number of electrons [see Fig. 3(a)]. Comparing Fig. 3(a) with Fig. 2(a), one sees that three new steps appear at $E_A\sim 0$, -1.5, and -7. As a matter of fact, there exists a new step at $E_A\sim -5$, but it is not resolved at current temperature $k_BT=0.01$. When the temperature becomes lower, this step will be resolved. Figure 3(b) provides the corresponding average occupation number of electrons at temperature $k_BT=0.1$. Apparently, with the temperature increasing, the electron occupation curve is smoothed and the new small steps seen in Fig. 3(a) are not resolved. In a recent work, Ramirez *et al.*[7] calculated the average occupation number of electrons for a similar double-QD system. Their results do not display the small steps associated with the interdot coupling [see Fig. 2(b) in Ref. 7]. Actually, this is what one expects, since the temperature used by them, $k_BT/U_A=0.04$, is even higher than the temperature for calculating Fig. 3(b), $k_BT/U_A=0.02$. For comparison, we also give in Figs. 3(d) and 3(f) the LDOS's corresponding to the average occupation number of electrons in Fig. 3(b). The LDOS's have appreciable changes as the temperature varies, but the main features are preserved. Finally, we present in Fig. 4 the average occupation number of electrons and the LDOS for the case with both strong-interdot coupling and strong-interdot Coulomb interaction. In this case, the spectral splittings are more clearly demonstrated. It is clear that all the small steps are well resolved [see Fig. 4(a)] and the LDOS peaks are largely separated [see Figs. 4(b) and 4(c)]. In addition, one can conclude that the LDOS depends appreciably on the electron occupation of the QD, since the LDOS exhibits apparent changes for different site energies of the dot.

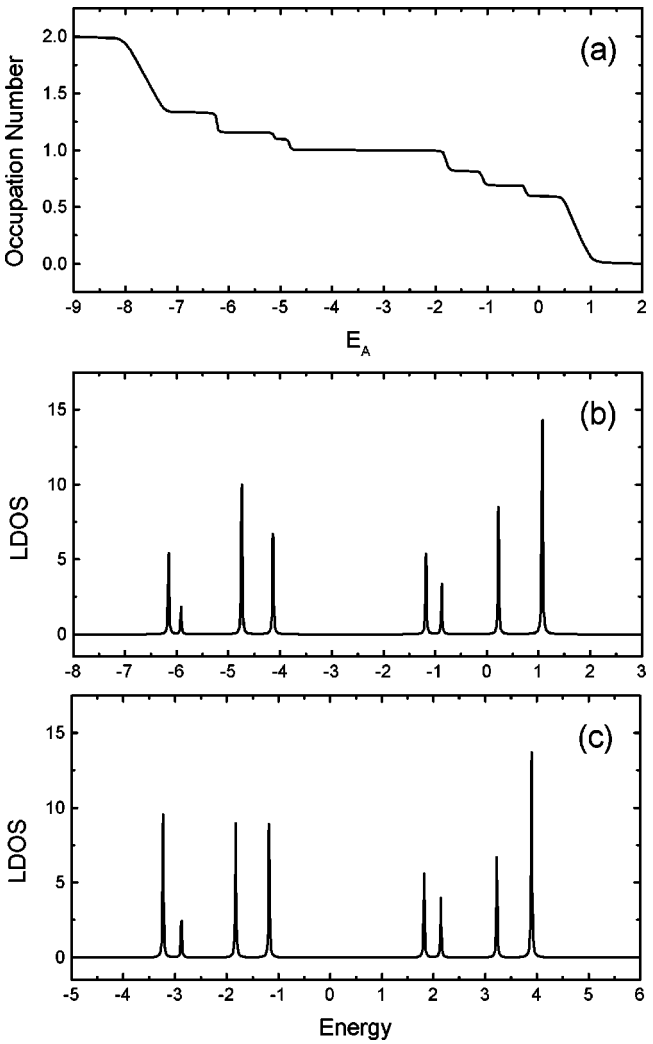

FIG. 4. (a) Average occupation number n_A as a function of the site energy E_A; (b) and (c) LDOS at dot A for $E_A=$ (b) -6 and (c) -3. Here $V_{AB}=1$, $T_{AB}=-1$, $k_BT=0.01$, and $\mu=0$. Other parameters are the same as in Fig. 1.

IV. SUMMARY

In summary, we have studied the spectral properties of a double-QD structure by a causal GF approach. To reveal the effects of electron correlations, we employ an Anderson-type Hamiltonian to model the double QD system in which both the intra and interdot Coulomb interactions, the interdot tunneling, and the dot-lead couplings are taken into account. The GF's are derived by an equation-of-motion method and the real-space RG technique. Numerical calculations show that the average occupation number of electrons in the QD exhibits staircase features and the LDOS has an appreciable dependence on the electron occupation of the dot. Our approach can be extended to artificial molecules with more than two coupled QD's. Though it is more complicated, the generalization is straightforward.

ACKNOWLEDGMENTS

This work was supported by the National Natural Science Foundation of China, the National Climbing Program of China, and K. C. Wong Education Foundation, Hong Kong.

*Electronic address: jqyou@red.semi.ac.cn

[1] For a review, see U. Meirav and E. B. Foxman, Semicond. Sci. Technol. **10**, 255 (1995).

[2] Y. Meir, N. S. Wingreen, and P. A. Lee, Phys. Rev. Lett. **66**, 3048 (1991).

[3] A. Groshev, T. Ivanov, and V. Valtchinov, Phys. Rev. Lett. **66**, 1082 (1991).

[4] S. Hershfield, J. H. Davies, and J. W. Wilkins, Phys. Rev. Lett. **67**, 3720 (1991).

[5] Y. Meir, N. S. Wingreen, and P. A. Lee, Phys. Rev. Lett. **70**, 2601 (1993).

[6] A. Levy Yeyati, A. Martin-Rodero, and F. Flores, Phys. Rev. Lett. **71**, 2991 (1993).

[7] F. Ramirez, E. Cota, and S. E. Ulloa, Superlattices Microstruct.

20, 523 (1996).
[8] T. Pohjola, J. König, M. M. Salomaa, J. Schmid, H. Schoeller, and G. Schön, Europhys. Lett. **40**, 189 (1997).
[9] T. Fujisawa, T. H. Oosterkamp, W. G. van der Wiel, B. W. Broer, R. Aguado, S. Tarucha, and L. P. Kouwenhoven, Science **282**, 932 (1998).
[10] R. H. Blick, D. W. van der Weide, R. J. Haug, and K. Eberl, Phys. Rev. Lett. **81**, 689 (1998).
[11] D. N. Zubarev, Usp. Fiz. Nauk **71**, 71 (1960) [Sov. Phys. Usp. **3**, 320 (1960)].
[12] S. W. Lovesey, *Condensed Matter Physics: Dynamic Correlations* (Benjamin/Cummings, Reading, 1980), p. 124.
[13] J. Hubbard, Proc. R. Soc. London, Ser. A **276**, 238 (1963).
[14] C. Lacroix, J. Phys. F **11**, 2389 (1981).
[15] K. Kang and B. I. Min, Phys. Rev. B **52**, 10 689 (1995).
[16] Q. Niu and F. Nori, Phys. Rev. Lett. **57**, 2057 (1986); Phys. Rev. B **42**, 10 329 (1990).
[17] J. Q. You, J. R. Yan, J. X. Zhong, and X. H. Yan, Europhys. Lett. **17**, 231 (1992).